Synaptic modifications driven by spike-timing-dependent plasticity in weakly coupled bursting neurons

Jian-Fang Zhou,[1,*] Wu-Jie Yuan,[1,†] Debao Chen,[1] Bing-Hong Wang,[2] Zhao Zhou,[1] Stefano Boccaletti,[3,4,‡] and Zhen Wang[5,§]

[1]*College of Physics and Electronic Information, Huaibei Normal University, Huaibei 235000, China*

[2]*Department of Modern Physics, University of Science and Technology of China, Hefei 230026, China*

[3]*CNR-Institute of Complex Systems, Via Madonna del Piano, 10, 50019 Sesto Fiorentino, Florence, Italy*

[4]*Unmanned Systems Research Institute, Northwestern Polytechnical University, Xi'an, 710072 Shanxi, China*

[5]*Center for OPTical IMagery Analysis and Learning (OPTIMAL), Northwestern Polytechnical University, Xi'an, 710072 Shanxi, China*

(Received 16 August 2017; revised manuscript received 26 January 2019; published 26 March 2019)

In the course of development, sleep, or mental disorders, certain neurons in the brain display spontaneous spike-burst activity. The synaptic plasticity evoked by such activity is here studied in the presence of spike-timing-dependent plasticity (STDP). In two chemically coupled bursting model neurons, the spike-burst activity can translate the STDP related to pre- and postsynaptic spike activity into burst-timing-dependent plasticity (BTDP), based on the timing of bursts of pre- and postsynaptic neurons. The resulting BTDP exhibits exponential decays with the same time scales as those of STDP. In weakly coupled bursting neuron networks, the synaptic modification driven by the spike-burst activity obeys a power-law distribution. The model can also produce a power-law distribution of synaptic weights. Here, the considered bursting behavior is made of stereotypical groups of spikes, and bursting is evenly spaced by long intervals.

DOI: 10.1103/PhysRevE.99.032419

I. INTRODUCTION

Certain cells in the brain (for instance thalamocortical [1–3], midbrain dopaminergic [4,5] and cortical [6–8] neurons) exhibit spike-burst activity during development [9,10], sleep [1,2], and mental disorders [3]. Such an activity behaves experimentally as a multi-time-scale phenomenon, with a slow process (burst) modulating a fast, repetitive, firing (spike) pattern. Several computational studies focused on the mechanisms producing spike-burst activity [11], on the dynamical synchronization in the coupled bursting neurons [12,13], and so on [14–17]. In particular, such a spike-burst activity is necessary to drive synaptic plasticity [9,10], whose study may help in understanding the modification and formation of synaptic weights. Recently, a lot of interest has been paid in experiments [18–21] and theories [22,23] of burst-timing synaptic plasticity.

Neural synapses have distinct properties of plasticity. In particular, spike-timing-dependent plasticity (STDP) was widely validated in experiments [24–28] and received much theoretical attention in recent years [29–33]. STDP is highly sensitive to correlations between pre- and postsynaptic firings [32,33], which contribute to learning, memory, and development [28,34,35], and could play an important role in synaptic modification evoked by neural spike-burst activity. Although self-organization of neural network through STDP has been extensively investigated in many computational studies [29–31], the synaptic modifications of neural networks instructed by spike-burst activity in the presence of STDP are not yet understood.

In this paper we cover this lack of knowledge, and study the role of spike-burst activity in instructing synaptic modifications, and in evolving the network structure through STDP. In particular, since it is experimentally known that synaptic conductance is weak during early development [36,37] and deep sleep [38,39], we here focus on unveiling (both numerically and analytically) the role of spike-burst activity in weakly coupled neurons. Our results may provide hints on the mechanism of distribution of synaptic weights.

II. MODEL

A. Coupled bursting neurons

We start by considering N coupled bursting neurons with chemical synapses. The model is composed of integrate-and-fire-or-burst (IFB) neurons [40], which are constructed by adding a slow variable to a classical integrate-and-fire model neuron. The IFB model can be easily used to control the timing of spike-burst activity for our research needs.

The dynamics of the membrane potential V_i of neuron i ($1 \leqslant i \leqslant N$) is described by the following equations [40]:

$$C\frac{dV_i}{dt} = I_i^{\mathrm{app}} - I_i^L - I_i^T + \sum_{j=1, j\neq i}^{N} gA_{ij}W_{ij}(V^E - V_i)\delta\left(t - t_{sp}^j\right), \quad (1)$$

$$\frac{dh_i}{dt} = \begin{cases} -h_i/\tau_h^- & (V_i > V^h) \\ (1-h_i)/\tau_h^+ & (V_i < V^h) \end{cases}. \quad (2)$$

*zhoujf2018@163.com
†yuanwj2005@163.com
‡stefano.boccaletti@gmail.com
§zhenwang0@gmail.com

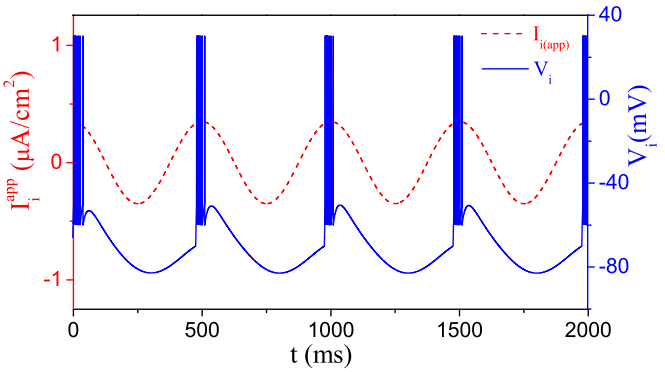

FIG. 1. The cosinusoidal applied current I_i^{app} with $\phi_i = 0$ and the membrane potential V_i for a single neuron i.

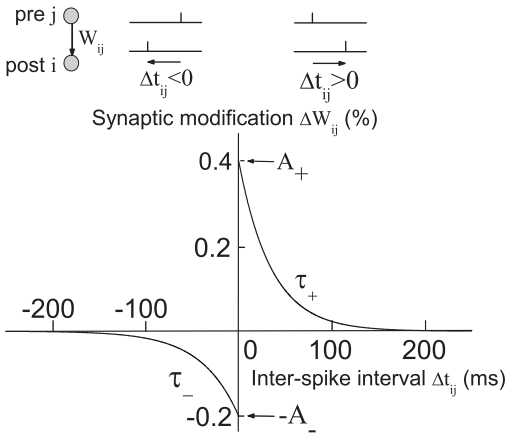

FIG. 2. Schematic illustration of the STDP modification function. Namely, synaptic strength W_{ij} from neuron j to i strengthens when the postsynaptic neuron i fires action potentials after presynaptic neuron j spikes (i.e., $\Delta t_{ij} \geqslant 0$), and weakens in the contrary case. STDP is modeled by exponential functions.

In Eq. (1), the currents include a cosinusoidal applied current, $I_i^{\text{app}} = I^0 \cos(2\pi f t + \phi_i)$; a constant conductance leakage current, $I_i^L = g^L(V_i - V^L)$; a low-threshold Ca^{2+} current, $I_i^T = g^T m_i h_i (V_i - V^T)$; and a coupling current $\sum_{j=1, j\neq i}^{N} g A_{ij} W_{ij} (V^E - V_i)\delta(t - t_{sp}^j)$. In Eq. (2), a slow variable h_i represents the inactivation of the low-threshold Ca^{2+} conductance, which involves T-type Ca^{2+} channels and produces the transmembrane current I_i^T. The characterization of the activation of I_i^T, $m_i = H(V_i - V^h)$, and $H(\cdot)$ is the Heaviside step function. In addition, C denotes the membrane capacity per unit area; g^L and g^T are the conductances for leakage and T-type Ca^{2+} channels; V^L and V^T are the corresponding reversal potentials; V^h is responsible for the activation of burst; τ_h^+ and τ_h^- set the durations of the burst and hyperpolarization.

In Eq. (1), the $\sum_{j=1, j\neq i}^{N} g A_{ij} W_{ij} (V^E - V_i)\delta(t - t_{sp}^j)$ stands for the currents received by the neuron i through the synapses from neurons j at their spike time t_{sp}^j. All neurons are considered to be excitatory, and the reversal potentials V^E for all the excitatory synapses are 0 mV. A simplified synaptic coupling of δ function is adopted. The parameter g is the synaptic conductance, reflecting the coupling strength. $A_{ij} (i \neq j)$ is an element of the adjacency matrix: $A_{ij} = 1$ when a synaptic connection exists from neuron j to i, and $A_{ij} = 0$ otherwise. $W_{ij} (i \neq j)$ accounts for the synaptic strength from neuron j to i, when the synapse exists (i.e., when $A_{ij} = 1$). Synaptic strengths are subject to a STDP rule, which will be described in the following subsection.

Each neuron i integrates the currents and inputs coming from the connected neurons j. When the potential V_i reaches the threshold value V^θ, the neuron i emits a spike, and then the membrane potential is reset to the value V^{reset}. In our simulations, we adopted the same parameter values as those in Ref. [40], which models relay neurons according to empirical observations. The parameters are given by $C = 2\ \mu\text{F/cm}^2$, $I^0 = 0.35\ \mu\text{A/cm}^2$, $f = 0.002$ KHZ, $g^L = 0.035$ mS/cm^2, $g^T = 0.07$ mS/cm^2, $\tau_h^- = 20$ ms, $\tau_h^+ = 100$ ms, $V^h = -70$ mV, $V^L = -75$ mV, $V^T = 120$ mV, $V^\theta = -50$ mV, and $V^{\text{reset}} = -60$ mV.

The burst timing is determined by the cosinusoidal applied current I_i^{app} [40]. As shown in Fig. 1, burst firings emerge in the ranges of large I_i^{app} close to the maximum I^0. The period of burst has the same value as that of I_i^{app} (i.e., $1/f$). The initial phase angle $\phi_i \in [-\pi, \pi)$ determines the starting time of a burst. As a consequence, the temporal order of pre- and postsynaptic bursts is determined by the difference of initial phase angles in paired neurons.

B. STDP

The STDP rule of synaptic weights (schematically represented in Fig. 2) captures actually the effects of temporal order of paired pre- and postsynaptic spikes [24,29], which in its turn determines whether the synapse is potentiated or depressed. The modification ΔW_{ij} of synaptic weight W_{ij} from postsynaptic neuron j to presynaptic neuron i is approximated by exponential functions of the time interval Δt_{ij} between post- and presynaptic spikes [32], described by

$$\Delta W_{ij} = \begin{cases} A_+ e^{-\Delta t_{ij}/\tau_+} & (\Delta t_{ij} \geqslant 0) \\ -A_- e^{\Delta t_{ij}/\tau_-} & (\Delta t_{ij} < 0) \end{cases} \tag{3}$$

The parameters A_+, A_-, τ_+, and τ_- account for the exponential properties of the STDP.

In our simulations, we model the STDP behavior by introducing internal variables $P_i(t)$ and $M_i(t)$ linked to the firing activity for each neuron i, and satisfying $\tau_+ \frac{dP_i}{dt} = -P_i$, and $\tau_- \frac{dM_i}{dt} = -M_i$.

Every time the neuron i fires an action potential at time t, $P_i(t)$ is incremented by A_+ and $M_i(t)$ is decremented by A_-. The synaptic weights W_{ij} for all the connected neurons j to the neuron i are modified according to $W_{ij} \to W_{ij} + P_j(t)$. If the change makes $W_{ij} > 1$, W_{ij} is set back to the maximal weight 1. Meanwhile, the synaptic weights W_{ji} are updated according to $W_{ji} \to W_{ji} + M_j(t)$. If this change makes $W_{ji} < 0$, W_{ji} is set to the minimal weight 0. Here, the parameters are given by $A_+ = 0.004$, $A_- = 0.002$, $\tau_+ = 35$ ms, and $\tau_- = 40$ ms.

III. RESULTS

For weakly coupled bursting neurons a weak synaptic coupling strength g is considered in our model. We focus on the role of the temporal interval of pre- and postsynaptic

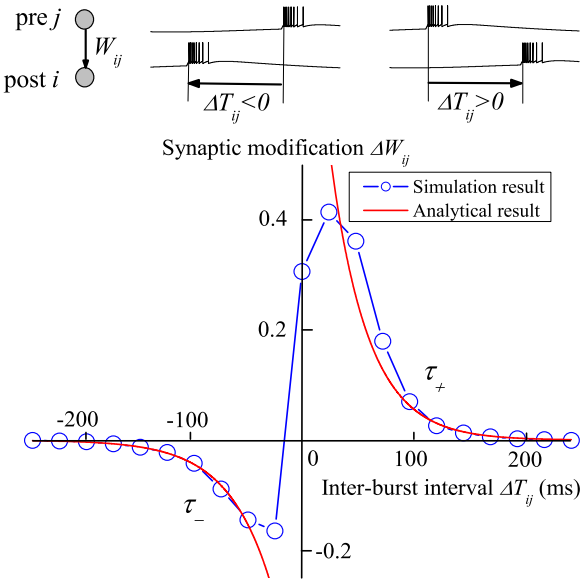

FIG. 3. The resulting BTDP modification function, i.e., the amount ΔW_{ij} of synaptic modification as a function of the interburst interval ΔT_{ij} after a simulation time of 2000 ms. Each synaptic weight is initialized at 0.5, and $g = 0.02$. For comparison, we also report the analytical result $4\Delta W_{ij}$ produced by $2000/(1/f) = 4$ "nearest-neighbor" pairings of burst firings, where the theoretical ΔW_{ij} are given by Eqs. (4) and (5). Here $R_i = R_j = 8/31$ KHZ and $T_b = 31$ ms are approximately obtained by the simulations.

bursts in instructing synaptic weights during the evolution towards their maximal value 1 (or minimal value 0), which will be attained asymptotically. To unveil self-organization and emergent properties during such evolution, we simulate the networks for a time of 2000 ms, i.e., when almost all evolved weights are still far away from their maximal or minimal values (this way avoiding boundary effects). The obtained statistic results do not depend qualitatively on the simulating time, as long as the weights are kept well away from their maximal or minimal values.

A. Effect of interburst interval

We focus on the case in which the coupling signal from synapses is very weak (weakly coupled networks). As a consequence, the spike-burst activity of the coupled neuron is almost independent on the coupling, and the temporal interval of pre- and postsynaptic bursts is approximately constant during the coupling course. First, we concentrate on the strong effects of the fixed interburst intervals on synaptic modifications in a two-neuron network with a synapse. The STDP related to pre- and postsynaptic spike activity is translated into burst-timing-dependent plasticity (BTDP), based on the timing of bursts of pre- and postsynaptic neurons. As shown in Fig. 3, ΔW_{ij} exhibits an exponential decay as a function of the interburst interval ΔT_{ij}, where the interval ΔT_{ij} is defined as the bursting time difference between post- and presynaptic neurons i and j. Remarkably, the decaying times have the same values τ_+ (when $\Delta T_{ij} > 0$) and τ_- (when $\Delta T_{ij} < 0$) as those of STDP.

Second, we move to analytic calculations. During the time T_b of a burst, the pre- and postsynaptic firing rates r_j and r_i are deemed to be approximated by the constant values R_j and R_i, respectively. Further, one estimates that the synaptic strengths are not close to their lower or upper limits and considers only the amount of synaptic weight induced by a "nearest-neighbor" pairing of bursts in pre- and postsynaptic neurons j and i. Pre- and postsynaptic neurons are assumed to start the bursts at the time $t = 0$ and $t = \Delta T_{ij}$, respectively.

When the burst of the presynaptic neuron precedes that of the postsynaptic neuron (i.e., $\Delta T_{ij} > 0$), the synaptic weight is strengthened. The amount of synaptic potentiation ($\Delta W_{ij} > 0$) can be calculated as

$$\begin{aligned}\Delta W_{ij} &= A_+ \int_{\Delta T_{ij}}^{\Delta T_{ij}+T_b} dt_i r_i(t_i) \\ &\quad \times \int_0^{T_b} dt_j r_j(t_j) e^{-(t_i-t_j)/\tau_+} \\ &= A_+ \tau_+^2 R_j R_i (e^{T_b/\tau_+} + e^{-T_b/\tau_+} - 2) e^{-\Delta T_{ij}/\tau_+} \\ &= k_P e^{-\Delta T_{ij}/\tau_+} \quad (\Delta T_{ij} > 0), \end{aligned} \tag{4}$$

where $k_P = A_+ \tau_+^2 R_j R_i (e^{T_b/\tau_+} + e^{-T_b/\tau_+} - 2)$.

Similarly, the depression ($\Delta W_{ij} < 0$) of synaptic weight when the burst of the postsynaptic neuron precedes that of the presynaptic neuron (i.e., $\Delta T_{ij} < 0$) is given by

$$\begin{aligned}\Delta W_{ij} &= -A_- \int_0^{T_b} dt_j r_j(t_j) \\ &\quad \times \int_{\Delta T_{ij}}^{\Delta T_{ij}+T_b} dt_i r_i(t_i) e^{-(t_j-t_i)/\tau_-} \\ &= -A_- \tau_-^2 R_j R_i (e^{T_b/\tau_-} + e^{-T_b/\tau_-} - 2) e^{\Delta T_{ij}/\tau_-} \\ &= -k_D e^{\Delta T_{ij}/\tau_-} = -k_D e^{-|\Delta T_{ij}|/\tau_-} \quad (\Delta T_{ij} < 0), \end{aligned} \tag{5}$$

where $k_D = A_- \tau_-^2 R_j R_i (e^{T_b/\tau_-} + e^{-T_b/\tau_-} - 2)$.

Clearly, Eqs. (4) and (5) verify the simulated exponential decays of the synaptic modification, with decaying times τ_+ (when $\Delta T_{ij} > 0$) and τ_- (when $\Delta T_{ij} < 0$) as a function of the interburst interval. Figure 3 indeed allows the reader to appreciate the consistency between simulation and analytical results. Moreover, one can see from Eqs. (4) and (5) that the impact of bursting (e.g., the burst duration T_b and the pre- and postsynaptic firing rates R_j and R_i) on the synaptic modification ΔW_{ij} is reflected by the strengths k_P and k_D of the exponential functions.

B. Power-law distributions in weakly coupled networks

Next, we study the distributions of probability densities of synaptic modifications and weights in weakly coupled networks with unidirectional and weighted connections (namely, A_{ij} and A_{ji}, as well as W_{ij} and W_{ji} are independent), consistent with the properties of chemical synapses. In our simulations, the initial phase angle ϕ_i is chosen randomly and independently for each i from a uniform distribution between $-\pi$ and π. Additionally, each initial synaptic weight is picked randomly and independently from a uniform density on [0, 1]. The total probability is counted in a bin 0.002 of synaptic modification (or synaptic weight) near ΔW (or W).

The results, presented in Fig. 4 for an Erdős-Rényi (ER) random network [41], do not depend substantially on the

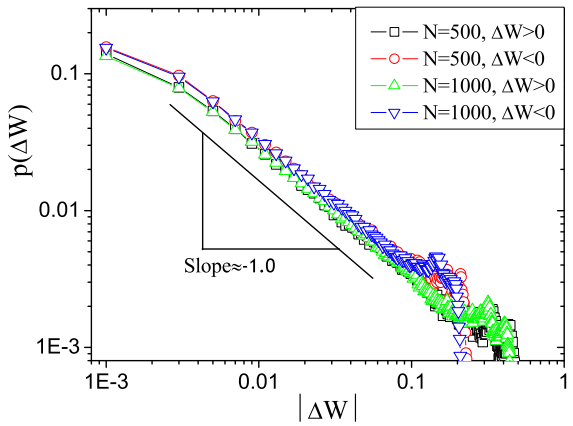

FIG. 4. Power-law fit of the middle part of probability distribution densities of synaptic modifications, for ER networks of different size N and connection probability 0.6. Data refer to both the synaptic potentiation (i.e., $\Delta W > 0$) and depression (i.e., $\Delta W < 0$). The solid line indicates the scale-free property with an approximate exponent of -1. $g = 0.0005$.

specific choices of initial conditions and used bins. The synaptic modification obeys a power-law distribution $p(\Delta W) \sim \mid \Delta W \mid^{-1}$ for both synaptic potentiation (i.e., $\Delta W > 0$) and depression (i.e., $\Delta W < 0$). Remarkably, such a scaling is the same for different size networks and for any network structures (not shown).

In the course of neural development, the initial synaptic weights are very weak and can be approximated as being zero [36,37]. When all initial weights are set to zero, the synaptic weight W follows a power-law distribution $p(W) \sim W^{-1}$, shown in Fig. 5. Once again, such a scaling is the same for different network sizes and different connecting topologies (not shown), indicating that the system organizes into a scale-free state. It is well known that STDP can lead to a bimodal distribution with synaptic strengths clustering both around zero and at the maximum synaptic weight [32,42]. The bimodal distribution of synaptic weights may appear in our model for long enough evolving time because most of the synaptic weights reach their maximal value 1 or remain at their minimal value 0. If most of synaptic weights do not reach the maximal value 1, the same power-law distribution as in Fig. 5 emerges for different evolving time (not shown).

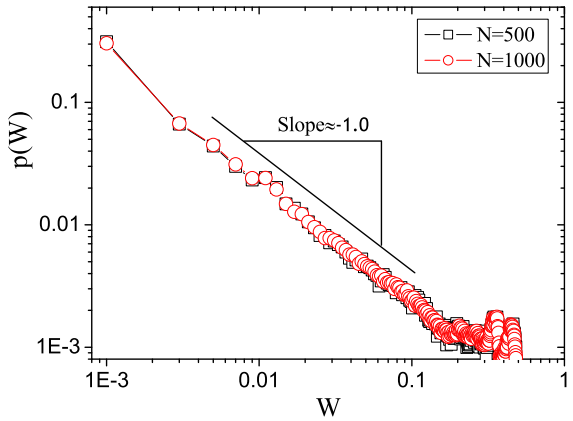

FIG. 5. Same as in Fig. 4, but for power-law fit of synaptic weights, with initial weights being zero.

Let us now focus on the theoretical analysis of $p(\Delta W)$ and $p(W)$. The value of ϕ_i completely determines the burst timing of neuron i in weakly coupled networks. Since each ϕ_i is a random number chosen uniformly from $-\pi$ to π, the distribution of interburst intervals ΔT is also uniform in the range of $\frac{1}{f}$-period time from $-1/2f$ to $1/2f$. In all the pairs of pre -and postsynaptic neurons with interburst interval $\Delta T > 0$ (i.e., $\Delta W > 0$), the probability that the pair j and i has an interburst interval ΔT_{ij} smaller than the certain ΔT is given by $P(0 < \Delta T_{ij} < \Delta T) = \frac{\Delta T}{1/2f} = 2f\Delta T$.

According to Eq. (4), the probability that the synaptic potentiation is larger than the value $\Delta W = k_P e^{-\Delta T/\tau_+}$ can be written as

$$P(\Delta W < \Delta W_{ij} < k_P) = -2f\tau_+ \ln(\Delta W/k_P).$$

The probability density $p(\Delta W)$ can then be calculated as $p(\Delta W) = -\frac{dP(\Delta W < \Delta W_{ij} < k_P)}{d(\Delta W)}$. One gets

$$p(\Delta W) = 2f\tau_+ (\Delta W)^{-1} \quad (\Delta W > 0). \tag{6}$$

Similarly, for $\Delta W < 0$, one can obtain the probability density $p(\Delta W)$ as

$$p(\Delta W) = 2f\tau_- \mid \Delta W \mid^{-1} \quad (\Delta W < 0). \tag{7}$$

When all the initial synaptic weights are 0, one gets $W = \Delta W$ and so the probability density $p(W)$ is naturally given by

$$p(W) = 2f\tau_+ W^{-1} \quad (W > 0). \tag{8}$$

One easily sees that all the distributions of probability densities follow a power-law scaling with an exponent of -1 in Eqs. (6)– (8), in perfect agreement with the simulations reported in Figs. 4 and 5. The conclusion of our theoretical analysis is that the essential ingredient to have a power-law scaling is an approximately fixed and uniform distribution of interburst intervals, resulting from weak connections in the network.

IV. CONCLUSION AND DISCUSSION

In summary, we numerically and theoretically investigated the synaptic plasticity evoked by the spike-burst activity in the presence of STDP. It was found that STDP is translated into BTDP, exhibiting exponential decays with the same time scales as those of STDP. Significantly, the resulting BTDP is not a new type of synaptic plasticity, but an expression of STDP induced by spike-burst activity. In weakly coupled bursting neuron networks, the synaptic modification driven by the spike-burst activity obeys a power-law distribution. In particular, our model can initially form power-law distribution of synaptic weights in weakly coupled networks, although a power-law distribution has been observed under STDP without bursting neurons in the literature [29]. Our results enlighten simple computational principles at the basis of the organization of synaptic weights in the presence of spike-burst activity.

Often, it is assumed that the synaptic weight distribution is exponential in certain brain areas [29]. Furthermore, some experimental results point towards a log-normal distribution

[43,44]. However, statistical tests [45] have revealed that a power-law distribution cannot be excluded at least for cortexL2(1), cortexL2(2), cortexL5(2), hippocampus, and cerebellum [29,42]. The stable power-law-like weight (or degree) distribution was observed by using STDP in some modeling studies [29,46–48]. Developing neural network is generated and modified by neural electrical activity, molecular cues, and gene expression [36]. Modern investigations have shown that neural electrical activity, characterized by spontaneous spike bursts in developing networks, plays an important role in forming synaptic weights during early and subsequent development [37,49]. Therefore, our results provide hints on the developing mechanism for the power-law distribution of synaptic weights. Indeed, the synaptic conductance is experimentally weak during early development [36,37], which is consistent with the hypothesis of weakly coupled networks adopted in our model. The time points and periods of distinct developmental processes (e.g., neurogenesis, migration, differentiation, synaptogenesis, apoptosis) differ in most species due to large differences in gestation periods [49,50]. Although the different structural developments of the cerebral cortex are more complex and are not well known during early stages, the hypothesis that synaptic weights are small and play a negligible role in the network dynamics during early development, which is considered in our model, cannot be all rejected on empirical grounds for all the species. Namely, the hypothesis is likely appropriate for certain species or local brain areas. Additionally, the maximal synaptic weight is selected as 1 and our simulating time is adopted by a short period (2000 ms), in order to reduce the calculation time. Selecting a large enough maximal weight, one can simulate the evolution of the network for a long enough time (corresponding to a long biological development time), and get the same qualitative results.

In our model, the considered bursting behavior is made of stereotypical groups of spikes, and bursting is evenly spaced by long intervals. The phase angles related to starting times of bursting are randomly and uniformly chosen in the region $[-\pi, \pi)$, which produces a random and uniform starting times of bursting for all the neurons. Since the resulting BTDP exhibits an exponential decays with the same time scales as those of STDP, the power-law distribution of synaptic weights arising from BTDP applies also to STDP for periodic spiking (no bursting) neurons with random and uniform firing times (the theoretical analysis is the same as for BTDP in the paper). It has been recently found that a periodic spatiotemporal spiking pattern (with randomly and uniformly chosen phase ordering) can give rise to a power-law distribution with an approximate exponent -1 in the middle part of the distribution [51], which is in full agreement with our result.

In our study, we considered only the initial weight change in weakly coupled networks, corresponding to the early stages of development. With the development of neurons, synaptic conductance maybe becomes large so that the connections of neural networks become strong. Strongly coupled networks will feature a strong interplay between structure and dynamics through STDP, possibly nonuniform distributions of the interburst intervals, and maybe richer distributions of synaptic weights. In addition, removal and rewiring of synapses is here not considered. Further investigations along these lines are expected to produce more realistic neural network structures and synaptic weight distributions.

Yet, our model studies the role of spike-burst activity in synaptic modification in weakly coupled networks. The resulting BTDP provides a simple computational principle for organizing synaptic weights driven by spike-burst activity in the presence of STDP. In particular, during sleep characterized by spike-burst neural activity, it has been experimentally found that memory is consolidated [38,52,53]. Our model and computational principle may provide a useful tip for the understanding of such sleep-dependent memory consolidation, which is still an unaddressed functional issue regarding the mechanism of synaptic modification.

ACKNOWLEDGMENTS

Work was partially supported by National Natural Science Foundation of China under Grants No. 11875031, No. U1803263, No. 61572224, No. 11005047, No. 11275186, No. 91024026, and No. 11505075; Natural Science Foundation of Anhui province under Grant No. 1508085MA04; Project of Natural Science in Anhui Provincial Colleges and Universities under Grants No. KJ2015ZD33 and No. KJ2016B006; Natural Science Foundation of Guangxi under Grant No. 2016GXNSFAA380202; and Scientific and Technological Activity Foundations for Preferred Overseas Chinese Scholar in Ministry of Human Resources and Social Security of China and in Department of Human Resources and Social Security of Anhui Province.

[1] M. Steriade, D. A. McCormick, and T. J. Sejnowski, Science **262**, 679 (1993).
[2] S. Postnova, K. Voigt, and H. A. Braun, J. Biol. Phys. **33**, 129 (2007).
[3] D. A. Hosford, S. Clark, Z. Cao, W. A. Wilson, F.-H. Lin, R. A. Morisett, and A. Huin, Science **257**, 398 (1992); O. C. Snead, Ann. Neurol. **37**, 146 (1995).
[4] A. S. Freeman, L. T. Meltzer, and B. S. Bunney, Life Sci. **36**, 1983 (1985).
[5] A. A. Grace and B. S. Bunney, J. Neurosci. **4**, 2866 (1984).
[6] M. E. Larkum, J. J. Zhu, and B. Sakmann, Nature (London) **398**, 338 (1999).
[7] C. P. J. de Kock and B. Sakmann, J. Physiol. **586**, 3353 (2008).
[8] S. R. Williams and G. J. Stuart, J. Physiol. **521**, 467 (1999).
[9] D. A. Butts, P. O. Kanold, and C. J. Shatz, PLoS Biol. **5**, e61 (2007).
[10] S. Marom and G. Shahaf, Rev. Biophys. **35**, 63 (2002); M. A. Corner, Brain Res. Rev. **59**, 221 (2008).
[11] V. N. Belykh, I. V. Belykh, M. Colding-Joergensen, and E. Mosekilde, Eur. Phys. J. E **3**, 205 (2000); E. M. Izhikevich, Int. J. Bifurcat. Chaos Appl. Sci. Eng. **10**, 1171 (2000).
[12] M. Dhamala, V. K. Jirsa, and M. Ding, Phys. Rev. Lett. **92**, 028101 (2004).

[13] I. Belykh, E. de Lange, and M. Hasler, Phys. Rev. Lett. **94**, 188101 (2005).
[14] R. Naud, B. Bathellier, and W. Gerstner, Front. Comput. Neurosci. **8**, 90 (2014).
[15] E. Hay and I. Segev, Cereb. Cortex **25**, 3561 (2015).
[16] A. S. Shai, C. A. Anastassiou, M. E. Larkum, and C. Koch, PLoS Comput. Biol. **11**, e1004090 (2015).
[17] R. Naud and H. Sprekeler, Proc. Natl. Acad. Sci. USA **115**, E6329 (2018).
[18] J. J. Letzkus, B. M. Kampa, and G. J. Stuart, J. Neurosci. **26**, 10420 (2006).
[19] B. M. Kampa and G. J. Stuart, J. Neurosci. **26**, 7424 (2006).
[20] R. C. Froemke, I. A. Tsay, M. Raad, J. D. Long, and Y. Dan, J. Neurophysiol. **95**, 1620 (2006).
[21] P. J. Sjöström, G. G. Turrigiano, and S. B. Nelson, Neuron **32**, 1149 (2001).
[22] P. Kaifosh and A. Losonczy, Neuron **90**, 622 (2016).
[23] J. Guerguiev, T. P. Lillicrap, and B. A. Richards, eLife **6**, e22901 (2017).
[24] G. Bi and M. Poo, J. Neurosci. **18**, 10464 (1998).
[25] S. Schuett, T. Bonhoeffer, and M. Hübener, Neuron **32**, 325 (2001).
[26] H. Yao and Y. Dan, Neuron **32**, 315 (2001).
[27] Y. Fu, K. Djupsund, H. Gao, B. Hayden, K. Shen, and Y. Dan, Science **296**, 1999 (2002).
[28] Y. Mu and M. Poo, Neuron **50**, 115 (2006).
[29] C. Meisel and T. Gross, Phys. Rev. E **80**, 061917 (2009).
[30] Y. K. Takahashi, H. Kori, and N. Masuda, Phys. Rev. E **79**, 051904 (2009).
[31] W.-J. Yuan, J.-F. Zhou, and C. Zhou, PLoS One **8**, e84644 (2013).
[32] S. Song, K. D. Miller, and L. F. Abbott, Nat. Neurosci. **3**, 919 (2000).
[33] B. Babadi and L. F. Abbott, PLoS Comput. Biol. **6**, e1000961 (2010).
[34] D. Feldman and M. Brecht, Science **310**, 810 (2005).
[35] D. Feldman, Annu. Rev. Neurosci. **32**, 33 (2009).
[36] K. Ganguly and M. Poo, Neuron **80**, 729 (2013).
[37] M. Munz, D. Gobert, A. Schohl, J. Poquérusse, K. Podgorski, P. Spratt, and E. S. Ruthazer, Science **344**, 904 (2014).
[38] U. Olcese, S. K. Esser, and G. Tononi, J. Neurophysiol. **104**, 3476 (2010).
[39] S. G. Horovitz, A. R. Braun, W. S. Carr, D. Picchioni, T. J. Balkin, M. Fukunaga, and J. H. Duyn, Proc. Natl. Acad. Sci. USA **106**, 11376 (2009).
[40] G. D. Smith, C. L. Cox, S. M. Sherman, and J. Rinzel, J. Neurophysiol. **83**, 588 (2000).
[41] P. Erdős and A. Rényi, Publ. Math. (Debrecen) **6**, 290 (1959).
[42] B. Barbour, N. Brunel, V. Hakim, and J.-P. Nadal, Trends Neurosci. **30**, 622 (2007).
[43] S. Song, P. J. Sjöström, M. Reigl, S. Nelson, and D. B. Chklovskii, PLoS Biol. **3**, e68 (2005).
[44] G. Buzsáki and K. Mizuseki, Nat. Rev. Neurosci. **15**, 264 (2014).
[45] A. Clauset, C. Shalizi, and M. Newman, SIAM Rev. **51**, 661 (2009).
[46] C.-W. Shin and S. Kim, Phys. Rev. E **74**, 045101(R) (2006).
[47] D.-P. Yang, H.-J. Zhou, and C. Zhou, PLoS Comput. Biol. **13**, e1005384 (2017).
[48] F. Effenberger, J. Jost, and A. Levina, PLoS Comput. Biol. **11**, e1004420 (2015).
[49] H. J. Luhmann, A. Sinning, J.-W. Yang, V. Reyes-Puerta, M. C. Stüttgen, S. Kirischuk, and W. Kilb, Front. Neural Circuits **10**, 40 (2016).
[50] Z. Molnár and G. Clowry, Prog. Brain Res. **195**, 45 (2012).
[51] S. Scarpetta, I. Apicella, L. Minati, and A. de Candia, Phys. Rev. E **97**, 062305 (2018).
[52] J. M. Siegel, Science **294**, 1058 (2001).
[53] S. Diekelmann and J. Born, Nat. Rev. Neurosci. **11**, 114 (2010).